L-19 **Wed. 18. 06., 12^{50}-13^{30}**

RIXS-MCD as a sensitive probe of 3d magnetism with hard x-rays

M. Sikora[1]*, A. Juhin[2] and P. Glatzel[3]

[1]*AGH University of Science and Technology, Academic Centre for Materials and Nanotechnology and Faculty of Physics and Appl. Comp. Sci., Al. Mickiewicza 30, 30-059 Krakow, Poland*
[2]*Institut de Minéralogie et de Physique des Milieux Condensés, CNRS and Université Pierre et Marie Curie, 4 Place Jussieu, 75252 Paris Cedex 5 France*
[3]*European Synchrotron Radiation Facility, CS 40220, 38043 Grenoble Cedex 9, France*

Keywords: magnetic moments, RIXS, RXES, XMCD

*e-mail: marcin.sikora@agh.edu.pl

The effect of magnetic dichroism was foreseen for x-ray absorption spectra (XAS) almost 25 years ago [1] and the first experimental observations of linear and circular x-ray magnetic dichroism (XMCD) spectra were subsequently reported [2]. Since then, it has turned into a common probe of element specific magnetization in para-, ferri- and ferro-magnetic systems, ranging from single atoms on surface, through molecular magnets to multilayers. At present XMCD is well understood and interpreted when measured at edges split by the spin-orbit coupling. For example, the 2*p* spin-orbit coupling gives rise to L_3 and L_2 edges providing convenient probe of 3*d* valence orbitals via the dipole-allowed $2p^6 3d^n \rightarrow 2p^5 3d^{n+1}$ transitions. XMCD at spin-orbit split edges enables simultaneous determination of spin and orbital magnetic moments upon application of the so-called "sum rules", which relate linear combinations of left and right circularly-polarized spectra to the ground state values of the magnetic moments of the absorber [3].

When applied to 3*d* transition metals and 4*f* rare earths, the main drawback of the technique is that the respective *L* and *M* absorption edges, that probe magnetic orbitals, lie in the soft x-ray range. Most soft x-ray magnetic circular dichroism (SXMCD) measurements employ total electron yield because significant self-absorption effects are observed when using total fluorescence yield detection. Thus, *L*-edge XMCD is mainly sensitive to the sample surface and, in addition, is not compatible with demanding sample environments such as high-pressure, liquid and gas cells, which limits the range of investigated materials and excludes *de facto* buried magnetic phases or multilayered samples. For these systems, the penetrating properties of hard X-rays are required, but at the *K*-edge the XMCD signal origin from the *p*-projected orbital magnetization density of unoccupied states, which is weak (~10^{-3} of the edge jump), difficult to interpret quantitatively, and do not allow for the separation of spin and orbital magnetic moments. The element specific studies of bulk magnetism and under extreme conditions have been largely limited to the very weak *K*-edge magnetic dichroism and to the Kβ emission spectroscopy [4-5]. However, the latter is sensitive to the spin and orbital kinetic moments (S and L) only, but not to the their orientation. As such, it does not provide quantitative information on the magnetic ordering and interactions.

Hence there is a need for a magnetic spectroscopic method in the hard x-ray range that can provide information on the ordering and the value of magnetic moments. We show that this goal can be achieved by coupling XMCD with 1*s*2*p* RIXS at the *K* pre-edge.

RIXS is a second-order optical process where first a core hole in a deep electron shell is created (intermediate state) that is replaced by a shallower core hole (final state). This results in sharper and often richer spectral features that origin from electron-electron and spin-orbit interactions. The 1*s*2*p* RIXS probes the evolution of $2p \rightarrow 1s$ emission (*K*α line) upon $1s \rightarrow p$ excitation (*K* absorption edge). If the incoming photon energy is in the range of *K* pre-edge, than a weak quadrupole $1s \rightarrow 3d$ excitations, possibly combined with some additional intensity due to dipole $1s \rightarrow 4p$ transitions shape the RIXS spectrum. Therefore, in 3*d* transition metals the 1*s*2*p* RIXS in the pre-edge rage probes predominantly the same final state ($2p^5 3d^{n+1}$) as the $L_{2,3}$ absorption edges, however using a hard x-ray photon in – photon out probe [6]. Combined with the idea of XMCD, i.e. using circularly polarized x-rays and external magnetic field, it becomes a promising technique to study 3*d* magnetic structure of transition metals.

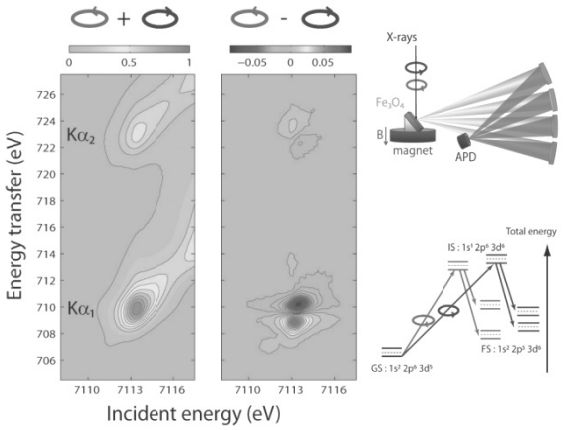

Figure 1. 1*s*2*p* RIXS (left) and RIXS-MCD (center) planes of bulk magnetite. In the right part the sketch of the experimental setup and the energy scheme of the transitions involved is shown. The energy transfer is the difference between incident and emitted photon energy (the total energy of the final state).

Figure 1 shows the experimental 1*s*2*p* RIXS-MCD plane on bulk magnetite at the Fe *K* pre-edge plotted as the difference between the spectra measured for left and right polarized light in comparison to the RIXS plane averaged over the two opposite photon helicities. It is apparent that only the resonant features give rise to the MCD effect, while the features due to non-resonant fluorescence (diagonal structures) do not show any detectable MCD. The spectra show a characteristic dispersion along incident photon energy, due to 1*s* hole lifetime broadening, and along the energy transfer, due to final state effects and 2*p* hole lifetime broadening. 1*s*2*p* RIXS-MCD reveals two groups of final states, which correspond to $K\alpha_1$ and $K\alpha_2$ emission lines, which are

composed mainly of two resonances with different spin polarization and opposite sign. The experimental data is compared with the theoretical RIXS-MCD calculated in the ligand field multiplet approach, where only the contribution of tetrahedral Fe^{III} was considered. The calculation involves an electric quadrupole excitation from $1s^2 2p^6 3d^5$ ground state to $1s^1 2p^6 3d^6$ intermediate state and electric dipole emission to $1s^2 2p^5 3d^6$ final state. It shows good agreement in terms of energy splittings and relative transition strengths of the left and right polarized channels. The only exception is the weak feature visible at 7112eV incident energy and 707eV energy transfer, that is ascribed to octahedral Fe^{II}. The theoretical model finds that the strong XMCD signal in 1*s*2*p* RIXS origin from combination of the exchange field and the 3d spin-orbit coupling in the intermediate state, that implies a different set of $1s^1 3d^6$ intermediate states to be reached from absorption of left and right handed circularly polarized x-rays. The splitting of the MCD features in horizontal and vertical direction is mainly given by the 3*d* spin-orbit coupling in the intermediate state and the 2*p*-3*d* Coulomb repulsions in the final state, respectively. The latter effect and the splitting induced by the 2*p* spin-orbit coupling act as an effective enhancer for the magnetic circular dichroism effect in 1*s*2*p*, that is at least one order of magnitude stronger than the XMCD observed in transmission. The intensity of $1s2p_{3/2}$ RIXS-MCD in bulk magnetite shows a peak-to-peak amplitude as large as 16% of the pre-edge maximum [7], that is comparable to the Fe L_3 edge XMCD [8,9].

The increase of intensity observed between *K*-edge XMCD and 1*s*2*p* RIXS-MCD is a significant advantage since it allows to measure data with better statistics. However, a strong enhancement is only expected for systems showing well defined pre-edge structures, such as oxides, molecular complexes etc… Indeed when 3*d* states are strongly hybridised with *p* states and heavily delocalised, such as in metals, it was observed experimentally that the gain in intensity is lost: for example in metallic Fe the intensity of RIXS-MCD was comparable to *K*-edge XMCD. However, it allows to separate the magnetic signal of metal sites and oxides of different formal valence states by tuning the energy transfer to the off-diagonal spectral features characteristic for a given oxidation state or site symmetry [10].

Ferro- and ferrimagnetic samples to which SXMCD would be blind (at least partially), such as buried layers, can readily be investigated using RIXS-MCD. For instance, high quality 1*s*2*p* RIXS-MCD signal was detected from a 40nm thick layer of magnetite buried under 60nm of Pt and Au. Another important observation was a significant reduction of the amplitude of the MCD signal in the thin layer to ~70% of the bulk value, which is in good agreement to the reduction of the saturation magnetization reported in literature [15]. Thus, the RIXS-MCD can be considered as a quantitative probe of net magnetization in thin layer samples. An interesting aspect of RIXS-MCD in comparison with *K*-edge XMCD is the possibility to select a region of the plane where the MCD effect is maximized for certain features of interest: for example, in the case of magnetite, the peak at 707eV energy transfer and 7112eV incident energy arises from octahedral Fe^{II}, while the double feature at 7114eV incident energy and 712eV energy transfer is dominated by the contribution from tetrahedral Fe^{III} . The RIXS plane can therefore be used to perform site-selective studies. By monitoring the changes as a function of space, pressure, temperature or time, RIXS-MCD can be adopted for element- and site-selective magnetometry and magnetic microscopy with hard x-rays. As an illustration, we show in Figure 2 the hysteresis loop measured on a thin buried layer of magnetite using a RIXS-MCD feature selectively for tetrahedral Fe^{III}, which is compared to the magnetization profile obtained with Vibrating Sample Magnetometer (VSM) .

Future studies of the dependence of RIXS-MCD on the direction of the wave-vector, the polarization vector, the magnetic field or the transfer momentum possibly combined with a polarization analysis of the scattered x-rays will enable to exploit the full potential of the technique.

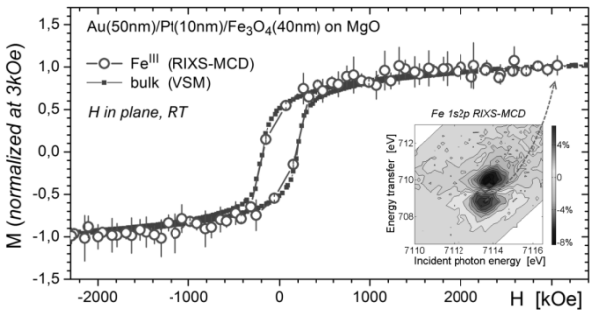

Figure 2. Element and site selective, Fe^{III} (T_d), hysteresis loop (circles) of a thin buried layer of magnetite compared to the VSM (small squares) results corrected for substrate signal.

Acknowledgments: We acknowledge ESRF for the provision of beam time. MS acknowledges support from Polish Ministry of Science and Higher Education and its grant for access to the ESRF facility.

[1] B. T. Thole *et al.*, *Phys. Rev. Lett.* **55** (1985) 2086.
[2] G. Schutz *et al.*, *Phys. Rev. Lett.* **58** (1987) 737.
[3] C. T. Chen *et al.*, *Phys. Rev. Lett.* **75** (1995) 152.
[4] J. Badro *et al.*, *Science* **300** (2003) 789.
[5] J. F. Lin *et al.*, *Nat. Geosci*. **1** (2008) 688.
[6] W. A. Caliebe *et al. Phys. Rev. B* **58** (1998) 13452.
[7] M. Sikora *et al.*, *Phys. Rev. Lett.* **105** (2010) 037202.
[8] D. J. Huang *et al.*, *Phys. Rev. Lett.* **93** (2004) 077204.
[9] C. Carvallo *et al.*, *Am. Mineral.* **93** (2008) 880.
[10] M. Sikora *et al.*, *J. Appl. Phys.* **111** (2012) 07e301.
[11] J. Orna *et al.*, *Phys. Rev. B* **81** (2010) 144420.